Doping dependence of femtosecond quasiparticle relaxation dynamics in $Ba(Fe,Co)_2As_2$ single crystals: Evidence for normal-state nematic fluctuations

L. Stojchevska,[1] T. Mertelj,[1] Jiun-Haw Chu,[2,3] Ian R. Fisher,[2,3] and D. Mihailovic[1]

[1]*Complex Matter Deptartment, Jozef Stefan Institute, Jamova 39, Ljubljana, SI-1000, Ljubljana, Slovenia*

[2]*Geballe Laboratory for Advanced Materials and Department of Applied Physics, Stanford University, Stanford, California 94305, USA*

[3]*Stanford Institute for Materials and Energy Sciences, SLAC National Accelerator Laboratory, 2575 Sand Hill Road, Menlo Park, California 94025, USA*

(Received 29 July 2011; revised manuscript received 5 July 2012; published 19 July 2012)

We systematically investigate the photoexcited (PE) quasiparticle (QP) relaxation and low-energy electronic structure in electron doped $Ba(Fe_{1-x}Co_x)_2As_2$ single crystals as a function of Co doping, $0 \leqslant x \leqslant 0.11$. The evolution of the photoinduced reflectivity transients with x proceeds with no abrupt changes. In the orthorhombic spin-density-wave (SDW) state, a bottleneck associated with a partial charge-gap opening is detected, similar to previous results in different SDW iron pnictides. The relative charge gap magnitude $2\Delta(0)/k_BT_s$ decreases with increasing x. In the superconducting (SC) state, an additional relaxational component appears due to a partial (or complete) destruction of the SC state proceeding on a sub-0.5-picosecond timescale. From the SC component saturation behavior the optical SC-state destruction energy, $U_p/k_B = 0.3$ K/Fe, is determined near the optimal doping. The subsequent relatively slow recovery of the SC state indicates clean SC gaps. The T dependence of the transient reflectivity amplitude in the normal state is consistent with the presence of a pseudogap in the QP density of states. The polarization anisotropy of the transients suggests that the pseudogap-like behavior might be associated with a broken fourfold rotational symmetry resulting from nematic electronic fluctuations persisting up to $T \simeq 200$ K at any x. The second moment of the Eliashberg function, obtained from the relaxation rate in the metallic state at higher temperatures, indicates a moderate electron phonon coupling, $\lambda \lesssim 0.3$, that decreases with increasing doping.

DOI: 10.1103/PhysRevB.86.024519 PACS number(s): 74.70.Xa, 78.47.jg, 75.30.Fv, 74.25.Dw

I. INTRODUCTION

Very soon after the discovery of high-temperature superconductivity in iron-based pnictides,[1–3] some unusual properties of the normal state were indicated by various experimental techniques[4–12] indicating a possible pseudogap.[5,6,8,10] More recently, the presence of the normal-state electronic nematic fluctuations[9,10,12–15] has been suggested from a remarkable anisotropy of physical properties induced by application of an external uniaxial stress in the tetragonal phase, well above the structural phase transition.

In comparison to the cuprates, where the pseudogap is ubiquitous, the existence of a pseudogap in iron-based pnictides is still controversial since no strong anomalies are present in the normal-state in-plane transport properties.[16,17] As in the cuprates, it is believed, that understanding the unusual normal state might be a key for revealing the origin of high-temperature superconductivity observed in these systems.

Time domain optical spectroscopy has been, among other spectroscopies, very instrumental in elucidating the nature of the unusual normal state in the cuprates by virtue of the fact that different components in the low-energy excitation spectrum could be distinguished by their different lifetimes.[18–24] In iron pnictides, several reports on photoexcited carrier dynamics exist,[8,25–32] but doping dependence studies are still incomplete.[26,28,32]

Here we present a systematic temperature (T) dependent time-domain optical spectroscopy study in $Ba(Fe_{1-x}Co_x)_2As_2$ spanning a large part of the x-T phase diagram from the undoped spin density wave (SDW) metallic state at $x = 0$ through coexisting superconducting-SDW state around $x = 5\%$, to the overdoped superconducting (SC) state at $x = 11\%$. We investigate the photoexcited quasiparticle relaxation in the low-T SDW and SC ground states as well as in the intermediate-T "pseudogap" state and the room-T metallic state.

From the temperature dependencies of the optical relaxation transients, we infer the relaxation bottlenecks, which we attribute to opening of the partial charge gap with the BCS-like temperature dependence in the orthorhombic state and the presence of a pseudogap-like suppression of the electronic density of states at higher temperatures. Surprisingly, we find that the twofold optical symmetry observed in the orthorhombic state persists well into the tetragonal state, suggesting association of the pseudogap-like behavior with a broken point symmetry and the presence of nematic fluctuations.

The analysis of the high-temperature relaxation dynamics experimentally confirms the supposition of a moderate electron-phonon coupling in iron-pnictide superconductors. We discuss separately the response of the SC state, where we observe an ultrafast nonthermal destruction of the SC condensate. The subsequent SC state recovery dynamics indicates clean gaps with the BCS-like temperature dependence.

The paper starts with presentation and description of experimental data in Sec. II, followed by a more detailed analysis and modeling, separately focusing on different regions of the phase diagram, in Sect. III. Conclusions and summary are presented in Sec. IV.

II. EXPERIMENTAL

A. Setup and samples

Single crystals of $Ba(Fe_{1-x}Co_x)_2As_2$ with Co dopings, $x = 0\%$, 2.5%, 5.1%, 7%, and 11%, were grown from a

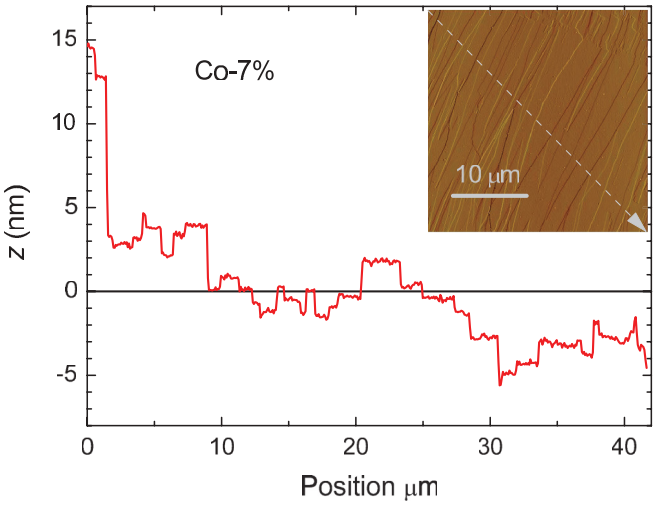

FIG. 1. (Color online) Atomic force microscope analysis of the cleaved surface quality in the near optimally doped Co-7% sample. The dashed arrow indicates the location of the plotted z profile.

self-flux, and characterized as described previously.[9,12,33] The Co-0% and Co-2.5% samples are underdoped and nonsuperconducting with SDW ordering while the Co-5.1% sample exhibits a coexistence of SDW and superconductivity at low T [see Fig. 2(e)]. The Co-7% and Co-11% samples correspond to the near optimally doped and overdoped regions of the SC phase diagram with no SDW ordering.

For optical measurements the crystals were glued onto a copper sample holder and cleaved by a razor before mounting in an optical liquid-He flow cryostat. Cleaving resulted in a terrace like surface (see Fig. 1) with a typical terrace width of a few micrometers and step height of a few nanometers. The relative orientation of the terraces with respect to the crystal axes was not determined.

Measurements of the photoinduced reflectivity, $\Delta R/R$, were performed using the standard pump-probe technique, with 50-fs optical pulses from a 250-kHz Ti:Al_2O_3 regenerative amplifier seeded with an Ti:Al_2O_3 oscillator. Unless otherwise noted, we used the pump photons with the doubled ($\hbar\omega_P = 3.1$ eV) photon energy and the probe photons with the laser fundamental 1.55-eV photon energy to easily suppress the scattered pump photons by long-pass filtering. In some cases, we used (for comparison) also the degenerate pump-photon energy of 1.55 eV. The pump and probe beams were nearly perpendicular to the cleaved sample surface with polarizations perpendicular to each other[35] and oriented with respect to the the crystals to obtain the maximum/minimum amplitude of the response at low temperatures. The pump and probe beam diameters were determined by measuring the transmittance of calibrated pinholes mounted at the sample place[36] resulting in 60 μm/50 μm and 70 μm/40μm for 3.1 eV/1.55 eV and 1.55 eV/1.55 eV pump/probe energies, respectively.

B. Overview of the experimental data set

In Fig. 2, we plot the temperature dependence of the raw photoinduced reflectivity ($\Delta R/R$) transients at different dopings. Despite that no deliberate uniaxial strain was applied to the samples,[9] all samples except the Co-11% sample showed a twofold rotational anisotropy with respect to the probe polarization below ~200 K (see Fig. 3).

In the orthorhombic state, the anisotropy indicates a preferential ordering of the orthorhombic twin domains in the probed volume. The anisotropy slightly varies along the surface of the samples with isolated spots that show almost no anisotropy. The transients of the less anisotropic spots are consistent with a linear combination of the most anisotropic transients. This indicates that the variation is not due to a sample inhomogeneity[37] but due to the spatially inhomogeneous detwinning.

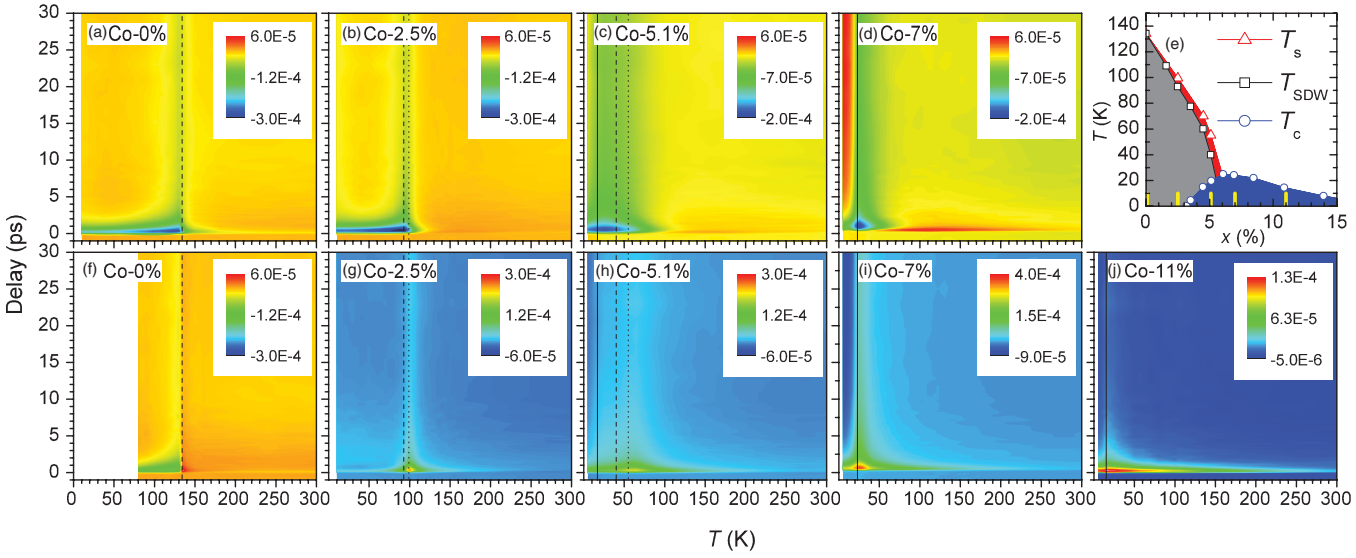

FIG. 2. (Color online) The photoinduced reflectivity ($\Delta R/R$) transients at 13 μJ/cm^2 pump fluence as a function of temperature at different dopings and probe polarizations (a)–(d), (f)–(j). The top row (a)–(d) corresponds to the $\mathcal{P}^-$ and the bottom row (f)–(i) to the $\mathcal{P}^+$ polarization. The vertical lines indicate T_c (full lines), T_{SDW} (dashed lines), and T_s (dotted lines). The phase diagram[33,34] of Ba($Fe_{1-x}Co_x$)$_2As_2$ (e). The investigated-sample dopings are marked by the yellow vertical bars.

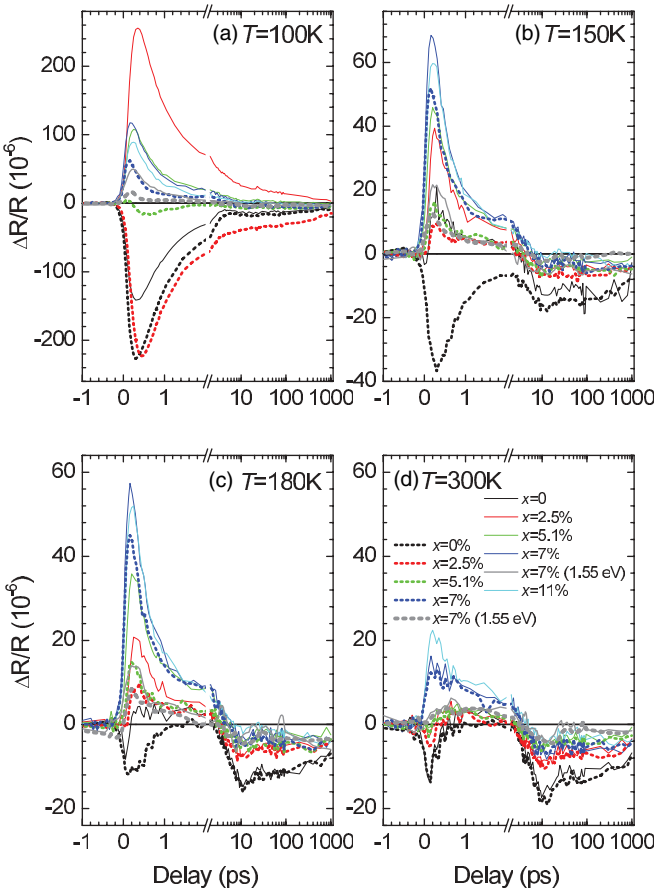

FIG. 3. (Color online) Anisotropy of the raw $\Delta R/R$ transients at a few representative temperatures as a function of Co doping x at 13 μJ/cm^2 pump fluence. The full and dotted lines correspond to $\mathcal{P}^+$ and $\mathcal{P}^-$ polarizations, respectively. The gray lines are the transients measured with 1.55 eV pump photon energy at 11 μJ/cm^2 in the Co-7% sample.

Since, according to the optical penetration depth in iron pnictides,[26] the probed volume is limited to a few tens of nanometers thick layer near the surface, we attribute the anisotropy to an anisotropic surface-strain bias presumably induced by the local pump-beam thermal load in the presence of the unidirectionally ordered terraces shown in Fig. 1. In the absence of information which crystallographic direction correspond to the two different orthogonal probe polarization, we denote the polarization corresponding to the low-temperature minimal and maximal subpicosecond peak $\Delta R/R$ value $\mathcal{P}^-$ and $\mathcal{P}^+$, respectively.

At any doping, the $\Delta R/R$ transients show a saturation with increasing pump laser fluence ($\mathcal{F}$) at low temperatures. At high temperatures, the saturation behavior vanishes as shown as an example for the Co-5.1% sample in Fig. 4.

C. Results in samples that show SDW ordering

The response in the undoped Co-0% sample is very similar to previous results in undoped $SrFe_2As_2$ and SmAsFeO.[26,29] Below $T_s = T_{SDW}$, the transients are dominated by the initial single exponential relaxation (see Fig. 3). At T_s, a slowing down of relaxation is observed in the form of a long-lived

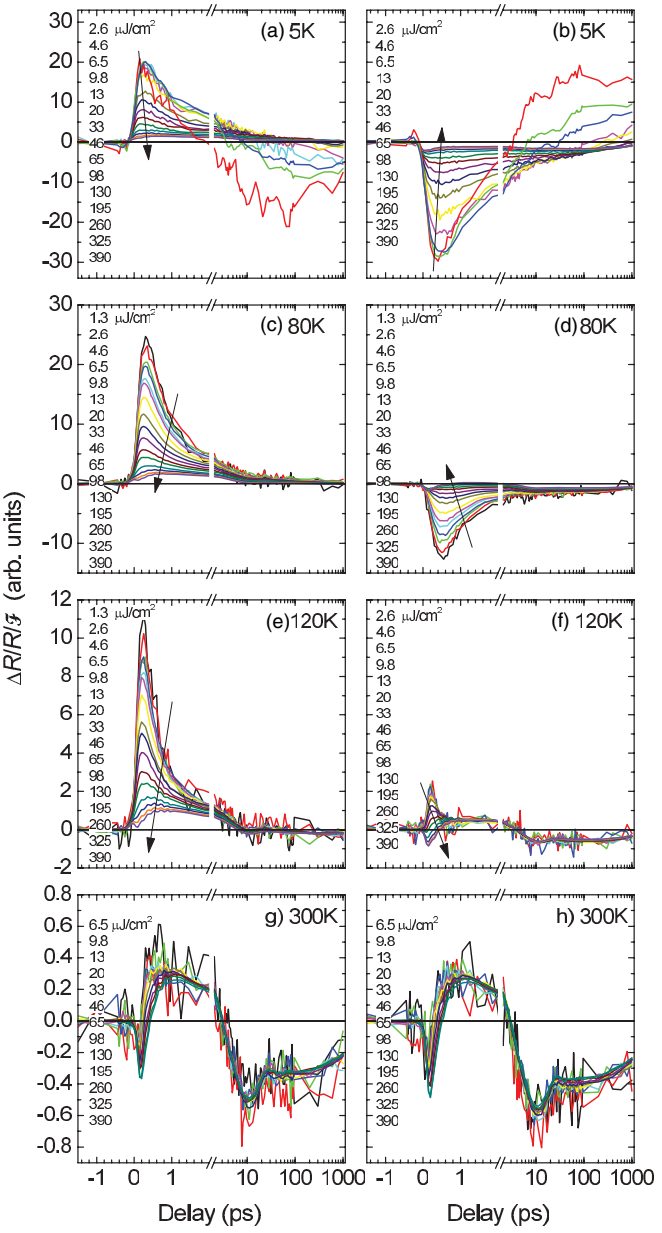

FIG. 4. (Color online) Fluence-normalized $\Delta R/R/\mathcal{F}$ transients as a function of $\mathcal{F}$ at different temperatures and probe polarizations in the Co-5.1% sample. The arrows indicate the direction of increasing $\mathcal{F}$. Overlapping curves indicate a linear $\mathcal{F}$ dependence. The left and right columns correspond to the $\mathcal{P}^+$ and $\mathcal{P}^-$ polarization, respectively.

relaxation, which is following the initial ~1.5 ps exponential decay and extends throughout the experimental nanosecond time window [see the $x = 2.5\%$ curves in Fig. 3(a)]. Above T_s, the amplitude of the initial subpicosecond relaxation strongly drops and the structure at around 10 ps, which was observed also in previously studied iron pnictides,[26,29] becomes apparent. The structure could be associated with the acoustic wave propagating into the sample after expansion of the excited volume due to the transient laser-pulse heating and will not be discussed further.

With increasing Co doping the anomalies around T_s become broader [see Fig. 5(a)] and the drop of the amplitudes with increasing T above T_s becomes slower. There are no clear

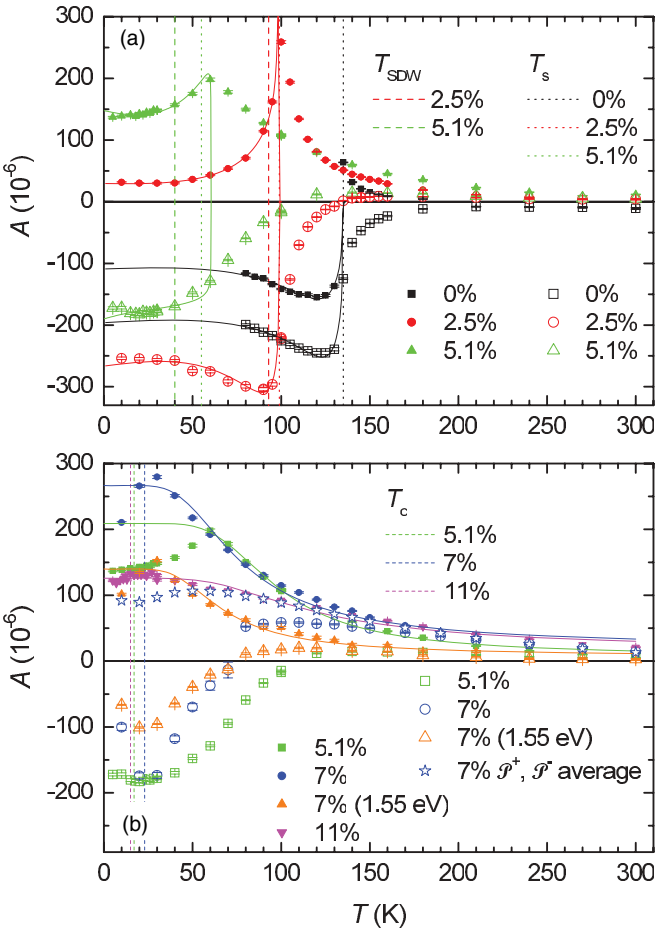

FIG. 5. (Color online) Amplitudes of the raw reflectivity transients as a function of temperature at different Co dopings, x, at 13 μJ/cm^2 pump fluence. The full and open symbols correspond to $\mathcal{P}^+$ and $\mathcal{P}^-$ polarizations, respectively. Open stars represent the amplitude of the probe-polarization averaged transients in the Co-7% sample. The thin lines in (a) are the fits of Eq. (4) discussed in text. The thin lines in (b) are the T-independent gap fits (6) discussed in text. The vertical lines indicate T_c (obtained from our optical data), T_{SDW}, and T_s (obtained from the phase diagram[33,34]).

separate features observed at the SDW transition temperature (T_{SDW}) in the Co-2.5% and Co-5.1% samples, where the SDW transition is split from the structural phase transition.

There is also a marked difference in the probe polarization anisotropy of the Co-0% sample with respect to the Co-2.5% and Co-5.1% samples where the amplitude shows either a peak for the $\mathcal{P}^+$ polarization or a step-like increase for the $\mathcal{P}^-$ polarization at T_s [see Fig. 5(a)]. This difference could be explained by a lower degree of detwinning due to the surface-strain bias in the Co-0% sample.

D. Results in superconducting samples

In the superconducting samples ($x > 2.5\%$), an additional SC component relaxing on a hundreds-of-picosecond timescale appears below the critical temperature (T_c) [see Figs. 6(a) and 6(b)]. The component is the most clearly observed at low pump fluences and has the largest magnitude in the optimally doped Co-7% sample [see Figs. 2(d) and 2(i)].

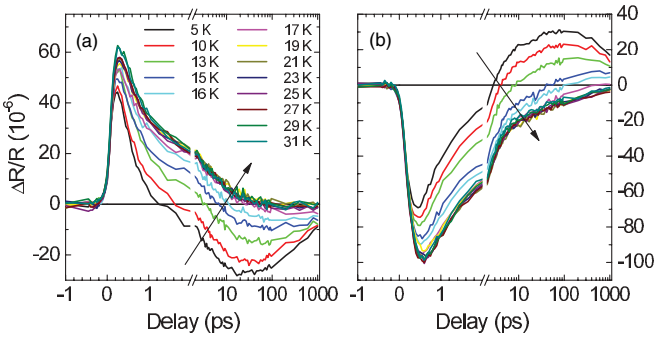

FIG. 6. (Color online) Low-temperature $\Delta R/R$ transients as a function of temperature in the Co-5.1% sample at 3.9 μJ/cm^2 pump fluence for two orthogonal probe polarizations $\mathcal{P}^+$ (a) and $\mathcal{P}^-$ (b). The arrows indicate the direction of increasing T.

As previously observed in the cuprates[36] and iron pnictides,[8,26] the SC component saturates at a lower pump fluence than the components that are present also above T_c. The saturation of the SC component is associated[8,26] with a complete SC state destruction in the optically probed volume.

In the normal state, the transients in the near-optimally-doped Co-7% sample show a similar temperature evolution as in the Co-5.1% sample above T_s, but shifted to lower temperatures. When cooling from the room temperature at ~70 K (~100 K in the Co-5.1% sample) the transients for the $\mathcal{P}^-$ polarization show an emergence of a negative picosecond component resulting in a change of sign together with appearance of the long-lived relaxation tail below ~50 K (~70 K in the Co-5.1% sample). There is, however, no structural transition with a peak of the amplitude as in the Co-5.1% sample at $T_s \simeq 60$ K, but a direct transition to the SC state at $T_c \simeq 23$ K.[38]

The transients in the overdoped Co-11% sample show, on the other hand, just a monotonous increase of the magnitude and relaxation timescale when the temperature is lowered from the room temperature down to the SC transition temperature similar to the probe polarization averaged transients in the Co-7% sample [see Fig. 5(b)].

III. ANALYSIS AND DISCUSSION

A. SC-state destruction and recovery

1. Fluence dependence

Due to a finite noise magnitude, we were able to investigate the $\mathcal{F}$ dependence of the SC component below the saturation fluence only in the nearly optimally doped sample ($x = 7\%$) with the highest $T_c \simeq 23$ K. At the lowest $\mathcal{F}$, the SC component dominates the raw $\Delta R/R$ transients [see Figs. 7(a) and 7(b)]. With increasing $\mathcal{F}$, however, the SC component quickly saturates while an increasing contribution of the normal state components starts to prevail at shorter timescales resulting in a shift of the minimum corresponding to the saturated SC component for the $\mathcal{P}^-$ probe polarization [see Fig. 7(a)] {and the maximum for the $\mathcal{P}^+$ probe polarization polarization [see Fig. 7(b)]} towards longer delays.

To extract the SC relaxation component we used the observation that the $\Delta R/R$ transients only weakly depend on the temperature just above T_c.[8,26] In Fig. 7(c), we show

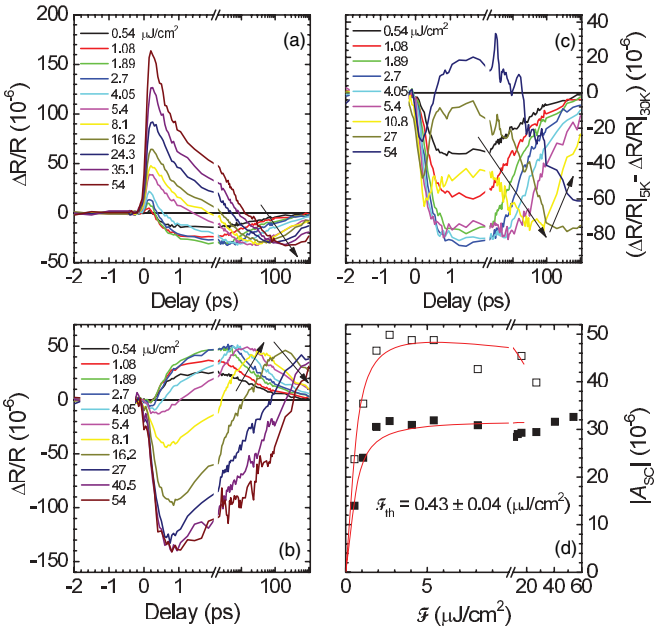

FIG. 7. (Color online) The raw $\Delta R/R$ transients in the optimally doped Co-7% sample as a function of $\mathcal{F}$ at $\mathcal{P}^+$ (a) and $\mathcal{P}^-$ (b) polarizations. The SC component as a function of $\mathcal{F}$ for the $\mathcal{P}^+$ polarization (c). The $\mathcal{F}$-dependence of the SC component amplitude for $\mathcal{P}^+$ (full symbols) and $\mathcal{P}^-$ (open symbols) polarizations in the optimally doped Co-7% sample (d). The thin lines in (d) are fits of the nonhomogeneous saturation model.[36] All data in this figure were obtained at $T = 5$K and 1.55 eV pump-photon energy. The arrows indicate the direction of increasing $\mathcal{F}$.

the $\mathcal{F}$-dependence of the SC component for the $\mathcal{P}^+$ probe polarization obtained by subtraction of the normal state $\Delta R/R$ transients measured above T_c (at 30 K) from the transients measured at 5 K. The subtraction procedure clearly fails at high $\mathcal{F}$ producing an apparent non-monotonous temporal dependence of the SC component at longer delays. The failure is attributed to the weak T dependence of the normal state components and/or a systematic error, which become large in comparison to the magnitude of the saturated SC component at higher $\mathcal{F}$. Nevertheless, one can observe an increasing duration of the plateau corresponding to the transient destruction of the SC state and slowing down of the subsequent SC state recovery with increasing $\mathcal{F}$.

We use the inhomogeneous SC-state destruction model[36] to fit $\mathcal{F}$ dependence of the SC component amplitudes [see Fig. 7(d)] and determine the SC state destruction threshold external fluence $\mathcal{F}_T = 0.43 \pm 0.04$ μJ/cm^2. Taking optical constants from Ref. 39, we obtain the reflectivity $R = 0.37$ and the optical penetration depth $\lambda_{op} = 34$ nm at the 1.55-eV pump photon energy, giving the bulk SC state destruction energy density required to completely destroy the superconducting state: $U_{p,Co-122}/k_B = \mathcal{F}_T(1-R)/\lambda_{op}k_B = 0.3$ K/Fe ($U_{p,Co-122} = 4.9$ J/mole). This value is much smaller than the energy necessary to heat the sample thermally to T_c, $U_Q/k_B = \int_{5\,K}^{T_c} c_p/k_B dT \simeq 2.4$ K/Fe ($U_Q = 40$ J/mole) indicating that the SC destruction is highly nonthermal. On the other hand, the thermodynamic condensation energy, $U_{c,Co-122}/k_B = 0.15 \pm 0.02$ K/Fe[40] is only half of $U_{p,Co-122}$ indicating that a half of the optical energy, initially completely absorbed by the electronic subsystem, is quickly (within $\tau_r \simeq 0.5$ ps) transferred to the subgap phonons, with $\hbar\omega_{ph} < 2\Delta_{SC}$, which can not break Cooper pairs.[41]

Comparing the destruction energy density with the near optimally doped SmAsFe(O, F) ($T_c \simeq 49$ K)[26] we find that it is much smaller than $U_{p,Sm-1111}/k_B = 1.8$ K/Fe. The ratio of the destruction energies $U_{p,Sm-1111}/U_{p,Co-122} = 6$ is, however, close to the ratio of the critical temperatures squared, $(T_{c,Sm-1111}/T_{c,Co-122})^2 = 4.5$, which corresponds to the ratio of the condensation energies if we assume a similar SC gap structure and the electronic density of states in both compounds.

2. Temperature dependence

To study the temperature dependence of the SC component we subtracted the average of the normal-state $\Delta R/R$ transients up to ~10 K above T_c from the raw transients. The resulting SC component is shown in Figs. 8(a)–8(e) for different Co dopings and polarizations. Due to a rather small signal to noise ratio, the $\mathcal{F}$-linear pump fluence region was not accessible so $\mathcal{F}$ was chosen significantly above the SC component saturation threshold in all cases.

The SC component shows a rise time of $\tau_r \lesssim 0.5$ ps followed by a plateau extending from tens of picoseconds at 5 K to several hundred picoseconds when the temperature is increased towards T_c.[42] As discussed above, the plateau corresponds to the transient destruction of the SC state. The timescale of the SC state recovery following the plateau is ~1 ns at 5 K and increases with increasing temperature.

Except in the overdoped Co-11% sample, which shows no polarization dependence of the $\Delta R/R$ transients and the smallest magnitude of the saturated SC component, the sign of the SC component changes for the two orthogonal probe polarizations. There is, however, no difference (within the experimental error) in the delay evolution of the SC component among the $\mathcal{P}^+$ and $\mathcal{P}^-$ polarizations. Taking into account, that different polarizations probe different parts of the Fermi surface,[15] this indicates that the destruction and the recovery of the SC order parameter is uniform along different parts of the Fermi surface.

In Fig. 8(f), we plot the temperature dependence of the SC-component saturated amplitude for all SC samples. The linear T dependence of the amplitude above T_c indicates some residual contribution due to the weak T dependence of the non-SC contributions. Below T_c, we observe (on top of the linear T dependence) the characteristic Mattis-Bardeen T dependence given by the high-frequency limit of the Mattis-Bardeen formula,[26,43]

$$\frac{\Delta R}{R} \propto \left[\frac{\Delta(T)}{\hbar\omega}\right]^2 \ln\left[\frac{3.3\hbar\omega}{\Delta(T)}\right], \qquad (1)$$

where $\hbar\omega$ is the probe-photon energy and $\Delta(T)$ the superconducting gap with the BCS temperature dependence.

3. Comparison with SmFeAs(O, F)

The presence of the plateau and the slow SC state recovery is different than in the near-optimally doped SmFeAs(O, F), where a two stage SC recovery was observed.[26] The fast

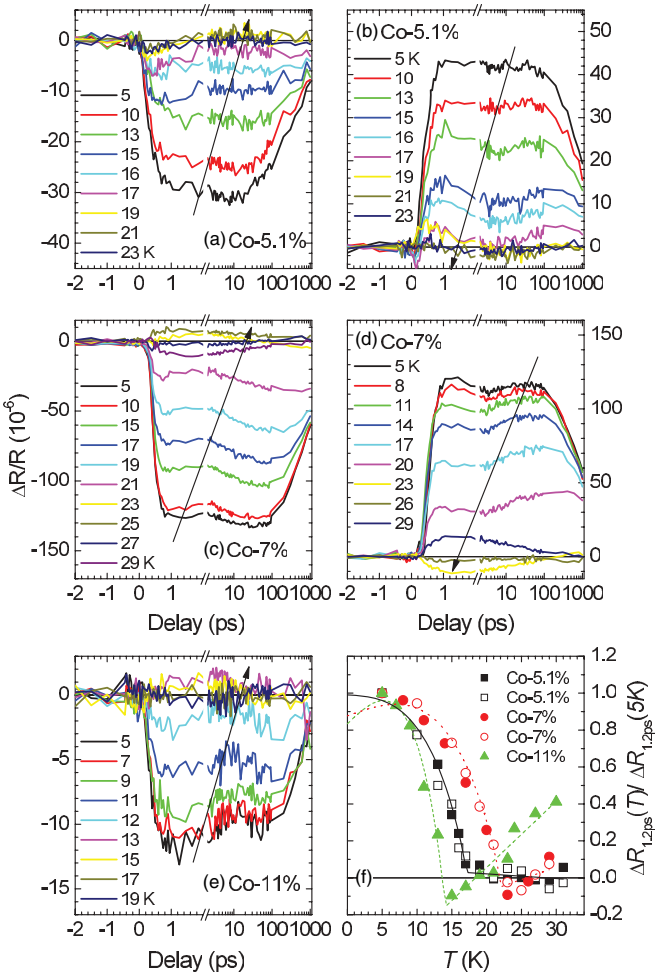

FIG. 8. (Color online) The superconducting responses at different polarizations in the Co-5.1% sample at 3.9 μJ/cm^2 pump fluence (a) and (b), in the Co-7% sample at 13 μJ/cm^2 pump fluence (c) and (d) and in the Co-11% sample at 2.6 μJ/cm^2 pump fluence (e). The normalized photoinduced reflectivity at 1.2 ps in all superconducting samples (f). Full and open symbols correspond to $\mathcal{P}^+$ and $\mathcal{P}^-$ probe polarizations, respectively. The lines in (f) are Mattis-Bardeen fits (1) discussed in text. The arrows indicate the direction of increasing T.

equilibration stage, appearing on a ~5 ps timescale in SmFeAs(O, F), corresponds to the initial local equilibration among all degrees of freedom and the slow, appearing on a several-hundred-picosecond timescale, corresponds to the energy escape from the optically probed volume by the diffusive heat transport.[26] The absence of the two-stage relaxation in $Ba(Fe_{1-x}Co_x)_2As_2$ is consistent with the fact, that, at the pump fluences used for the T-scans, the total laser energy deposited in the optically probed volume corresponds to heating the sample to a temperature well above T_c, in the 30–40 K range. The sample thus remains in the normal state after the fast stage and the SC recovery is governed by the diffusive-heat-transport slow stage only.

Moreover, in the present case a separate two-stage relaxation is not observed even at the lowest $\mathcal{F}$ just above the threshold [see Fig. 7(c)] suggesting that the initial local equilibration is slower than in SmFeAs(O, F). This could be ascribed to virtually clean SC gaps[44] in the case of $Ba(Fe_{1-x}Co_x)_2As_2$ (and other 122 systems[26]) in comparison to SmFeAs(O, F) where the relaxation dynamics and a large low-T heat capacity[45] suggest the presence of ungapped parts of the Fermi surface in the SC state.[26]

B. Orthorhombic SDW state

1. Determination of the relaxation components

While in the Co-0% sample at low T the initial relaxation can be fit with a single exponential decay in both polarizations the samples with finite Co dopings clearly show a multi-component relaxation. In order to consistently fit the transients for both probe polarizations up to 100 ps delay, to determine T dependencies of relaxation times, three exponentially decaying components need to be employed:[46]

$$\frac{\Delta R}{R} = \sum_{i\in\{A,B,C\}} \frac{A_i}{2} e^{-\frac{t-t_0}{\tau_i}} \operatorname{erfc}\left[\frac{\sigma^2 - 4(t-t_0)\tau_i}{2\sqrt{2}\sigma\tau_i}\right] + \frac{A_0}{2}\operatorname{erfc}\left[\frac{\sqrt{2}(t_0-t)}{\sigma}\right], \quad (2)$$

where σ corresponds to the effective width of the excitation pulse with a Gaussian temporal profile arriving at t_0 and τ_i the exponential relaxation times. The last term in Eq. (2) accounts for slower processes, which are not of interest here. During the fitting, the relaxation times for the two orthogonal polarizations were linked while amplitudes were kept independent.

Component A (see Fig. 9) with relaxation time $\tau_A \sim 0.2$ ps is needed to fit the difference in the rise time dynamics between the two orthogonal probe polarizations. The component is absent in the Co-0% and superconducting Co-11% samples and appears below ~150 K in the other samples [see Figs. 10(a) and 10(b)] with the relaxation time only weakly dependent on the temperature. It could be associated with the initial relaxation of the high-energy optically excited electrons towards the Fermi energy and/or the interband momentum scattering between states near the Fermi energy at different parts of the Fermi surface.[47]

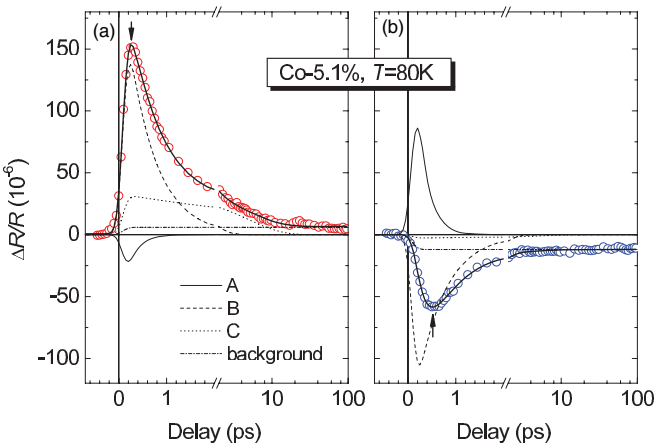

FIG. 9. (Color online) An example of the three-exponential fit (2) for the Co-5.1% sample for (a) $\mathcal{P}^+$ and (b) $\mathcal{P}^-$ polarizations. Note the different rise-time dynamics for the two polarizations resulting in different delays of the extrema indicated by arrows.

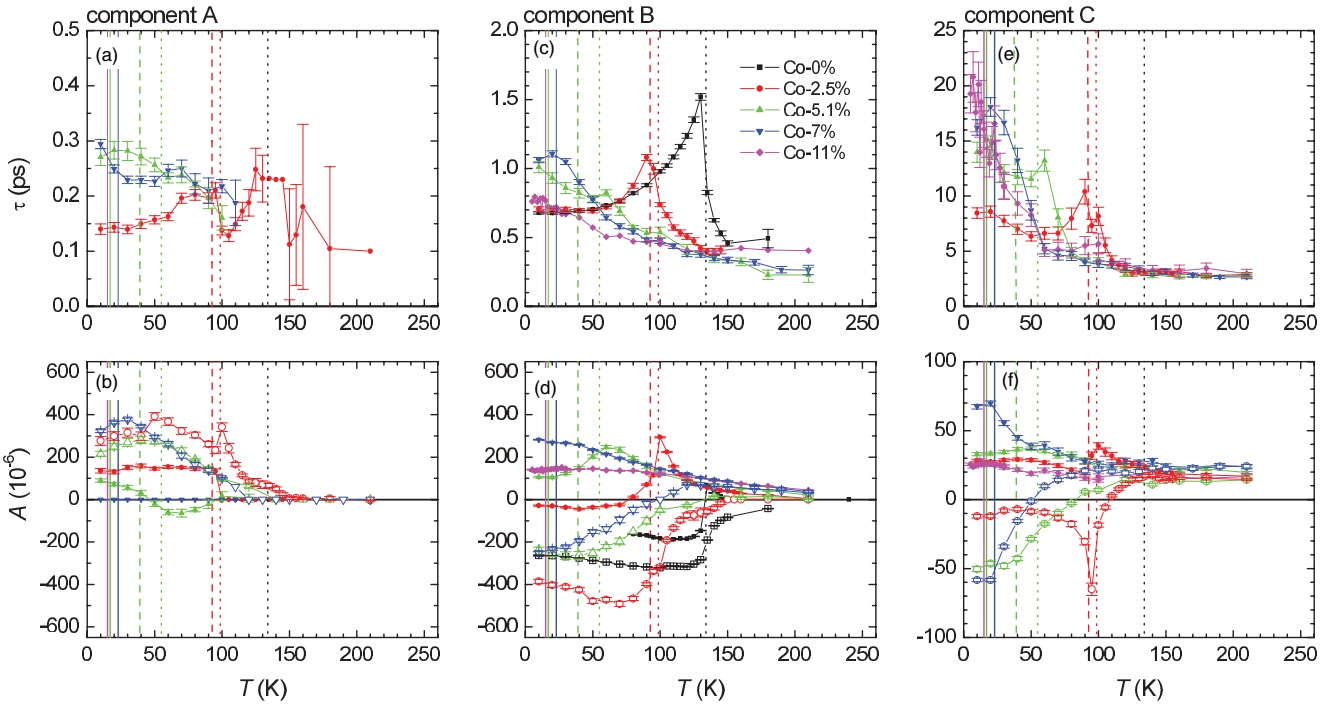

FIG. 10. (Color online) Multiexponential fit relaxation times (a), (c), (e), and corresponding amplitudes (b), (d), (f). The empty and filled symbols represent $\mathcal{P}^+$ and $\mathcal{P}^-$ probe polarizations, respectively. The vertical lines indicate T_c (full lines), T_{SDW} (dashed lines), and T_s (dotted lines).

Component B is the main component present in all samples [see Fig. 10(d)] representing the initial 0.3–1.5 ps decay. The relaxation time τ_B [see Fig. 10(c)] shows a slowing down[48] at T_s in the samples with the SDW order. The peak in τ_B is only weakly pronounced in the Co-5.1% sample, which shows the SDW-SC coexistence, and is completely absent in the Co-7% and Co-11% samples, where we observe a monotonous increase of τ_B with decreasing temperature.[49]

Component C [see Figs. 10(e) and 10(f)] has the longest relaxation time (τ_C) spanning from a few ps at 200 K up to 20 ps at 5 K in the Co-7% and Co-11% samples.[50] In the Co-2.5% and Co-5.1% samples, τ_C also slows down near T_s. The qualitative behavior of this component is very similar to component B so it is very likely that both components together are due to a single process with a nonexponential decay dynamics.

2. *Analysis of the temperature dependence*

Below T_s, the $\Delta R/R$ amplitude shows different T dependence for the two orthogonal probe polarizations, which is most clearly pronounced in the Co-2.5% sample [see Fig. 5(a)]. This indicates that the states involved in the two orthogonal probe polarizations correspond to different parts of the Fermi surface,[51] presumably originating from different bands crossing the Fermi energy as confirmed by the recent ARPES photon-polarization analysis in untwinned $Ba(Fe_{1-x}Co_x)_2As_2$.[15]

To analyze the anisotropic T dependence, we first rewrite Eq. (4) from Ref. 52, that describes the photoinduced reflectivity change due to the presence of photoexcited carriers, in a more general form for a pair of bands:

$$\Delta R_{\alpha,\beta} \propto \int \mathrm{d}^3k[|M_{\alpha,\beta}(\mathbf{k})|^2 \Delta f_\alpha(\mathbf{k}) \times g(\epsilon_\beta(\mathbf{k}) - \epsilon_\alpha(\mathbf{k}) - \hbar\omega_{\mathrm{probe}})]. \quad (3)$$

Here, $M_{\alpha,\beta}$ is the effective probe-polarization dependent optical-dipole matrix element between an initial band, α, and a final band, β, $\Delta f_\alpha(\mathbf{k})$ the photoexcited change of the charge-carrier distribution function in the initial band, $g(\epsilon)$ the effective transition line shape and $\hbar\omega_{\mathrm{probe}}$ the probe photon energy. For simplicity, we assumed that the energy of the final band is far from the Fermi energy, $|\epsilon_\beta(\mathbf{k}) - \epsilon_F| \sim \hbar\omega_{\mathrm{probe}} \gg k_B T$, so $\Delta f_\beta(\mathbf{k})$ can be neglected after the fast initial relaxation of the ultrahot carriers.

Integral (3) selectively samples $\Delta f_\alpha(\mathbf{k})$ in different regions of k space depending on the probe polarization and photon energy. Due to contributions of several optical transitions with finite effective linewidths it is usually assumed that Eq. (3) smoothly samples over the relevant energy range in the vicinity of the Fermi energy and ΔR can be approximated by the total photexcited carrier density, $\Delta R = \gamma n_{\mathrm{pe}}$,[52,53] and any change of ΔR upon change of external parameters (T for example) is attributed to the change of n_{pe} while the proportionality factor γ is assumed to be a constant.

In $Ba(Fe_{1-x}Co_x)_2As_2$, however, a complex band structure reorganization with bands shifting by as much as 80 meV has been observed below T_s.[15] These shifts can significantly modify the sampling region of the integral (3) and violate the assumption of a constant γ. To take this into account, we therefore assume that γ is temperature dependent and expand it in terms of an order parameter. The order parameter

TABLE I. Charge gap magnitudes in the SDW samples and characteristic pseudogap energies in the SC samples as obtained from the fits in Fig. 5 discussed in text.

x	$2\Delta(0)/k_BT_s$	$2\Delta_{PG}$ (K)
0%	9 ± 2	...
2.5%	7 ± 2	...
5.1%	4 ± 2	800 ± 100
7%	...	660 ± 100
11%	...	610 ± 100

can be associated with the opening of a partial T-dependent charge gap $\Delta(T)$ upon the Fermi surface reconstruction below T_s.[54] Assuming a complex BCS-like order parameter with the magnitude $\Delta(T)$ below T_s, we obtain

$$\Delta R = [\gamma_0 + \eta\Delta(T)^2]n_{pe}. \quad (4)$$

Since for the $\mathcal{P}^-$ probe polarization the T-dependent $\Delta R/R$ amplitude shows the characteristic shape that is associated with an appearance of a bottleneck in the photoexcited electron relaxation below T_s we use the bottleneck model from Kabanov *et al.*,[53]

$$n_{pe} \propto 1 \Big/ \left\{ \left[\Delta(T) + \frac{k_BT}{2} \right] \times \left[1 + g_{ph}\sqrt{\frac{k_BT}{\Delta(T)}} \exp\left(-\frac{\Delta(T)}{k_BT} \right) \right] \right\}, \quad (5)$$

to describe T dependence of n_{pe}. Using the BCS temperature-dependent gap we can obtain a good fit of Eq. (4) to the $\Delta R/R$ amplitude for both probe polarizations (see Fig. 5). The relative gap magnitudes are consistent (see Table I) with previously reported values[29] in different iron pnictides and show a decrease with doping, consistent with a decrease of the stability of the orthorhombic SDW state. Similarly to ReFeAsO,[55] the onset of the partial gap opening can be associated with the structural and not SDW transition.

C. Normal state

1. Normal state bottleneck and pseudogap

Above T_s, the T-dependent $\Delta R/R$ amplitude shows tails that can not be described by Eq. (5). These tails indicate a bottleneck in relaxation and therefore the presence of a pseudogap persisting up to ~200 K. With increasing Co doping the bottleneck becomes even more pronounced at higher T and remains present also in the non-SDW Co-7% and Co-11% samples.

The $\mathcal{F}$ dependence of the $\Delta R/R$ transients shown in Figs. 4(e) and 4(f) indicates that at high excitation the relaxation component, which is responsible for the tails, saturates and the shapes of transients become almost identical to the room temperature ones. The observed external saturation fluences of the order of 100 μJ/cm^2 correspond to the absorbed optical energy of ~50 K/Fe. This amount of energy would thermally heat the experimental volume for only a few K. Any property or a state, that is responsible for the tails, can therefore be nonthermally destroyed. This rules out any static effect, such as the surface-strain bias, a rigid band shift with T or a band-structure pseudogap, for example, as possible origins of the tails.

To obtain a quantitative information about the pseudogap, we analyze the normal state T-dependent $\Delta R/R$ magnitude in the context of the relaxation across a T-independent gap.[8,26,53] Assuming that in the normal state any T dependence of γ can be neglected, we fit the $\mathcal{P}^+$ $\Delta R/R$ magnitude[56] by

$$\Delta R \propto n_{pe} \propto \left\{ 1 + g_{ph} \exp\left[-\frac{\Delta_{PG}(T)}{k_BT} \right] \right\}^{-1}, \quad (6)$$

where g_{ph} is the ratio between the number of involved phonons and the number of involved quasiparticle states.[53]

The obtained pseudogap magnitudes $2\Delta_{PG}$ (see Table I) are very similar to spin pseudogap magnitudes obtained from T dependence of the Knight shift[6] suggesting that a suppression of density of states in the fluctuation region is present in both, spin and charge, densities of states. The presence of the charge pseudogap is supported also by the T dependence of the c-axis electrical resistivity[11] and the V shape of the tunneling conductance spectra.[10]

It should be noted that the charge pseudogap was observed also in the electron doped SmFeAs(O, F),[8,26] which, similarly to $Ba(Fe_{1-x}Co_x)_2As_2$, shows the spin pseudogap.[5]

2. Anisotropy and nematic fluctuations

One of the most striking features of our data set is the observation of the twofold in-plane rotational anisotropy of the optical transients in the tetragonal phase (see Fig. 3), well above T_s, without any deliberately applied external uniaxial stress. The absence of the anisotropy at the room temperature and in the Co-11% sample proves that the observed anisotropy is not an experimental artifact but is intrinsic to our samples. At low dopings, the high-T anisotropy axes match the orthorhombic-state anisotropy axes indicating that also the high-T anisotropy is oriented along the orthorhombic crystal axes direction. Moreover, the change of the sign of the SC component in Co-5.1% and Co-7% samples is a strong indication that the anisotropy originates from the bulk of the probed volume and not from the edges of the teraces.

In the absence of any structural data that would indicate that our samples are not tetragonal in the thermodynamic equilibrium above T_s, we assume that the breaking of the fourfold tetragonal symmetry is not spontaneous, but is a consequence of anisotropic boundary and/or excitation conditions that introduce an anisotropic surface strain.

We believe that the strain is a consequence of the local crystal expansion due to the local thermal load. The anisotropy of the strain could be linked to the unidirectional terraces observed on the surface of the cleaved crystals. The strain is expected to be weak since the average increase of the temperature in the experimental volume is at most a few K. The anisotropic response of the sample is therefore possible only if the system is very close to a spontaneous symmetry-breaking instability of the fourfold rotational symmetry.

Since the reflectivity is a second rank tensor, the observed twofold anisotropy can not distinguish between the twofold in-plane rotational symmetries and the absence of any rotational symmetry (C_1). The observed twofold anisotropy is therefore compatible with a nematic order parameter[57] as well as with

an in-plane antiferromagnetic (AF) ordering and even in-plane ferro orderings. Since photons do not directly couple to spins the observation of AF fluctuations in optical response is at best of second order and therefore very unlikely. Moreover, there is no appreciable external magnetic field to order spins and the anisotropy is a continuous function of temperature with a clear anomaly at T_s and no anomaly at T_{SDW} in Co-2.5% and Co-5.1% samples. We therefore tentatively associate the twofold symmetry breaking instability with nematic fluctuations or ordering of the Fe d orbitals. The ordering is not necessary static at all temperatures since the timescale of relaxation is below ∼0.5 ps. Similar nematic ordering, albeit static in the presence of an external uniaxial strain and at somewhat lower temperatures, was observed also by other techniques.[9,10,12,15]

Due to the concurrent appearance of the bottleneck and the polarization anisotropy of the transients around 200 K the pseudogap might be associated with the nematic fluctuations responsible for the fourfold rotational symmetry breaking. The fluctuations appear to be particularly strong in the Co-5.1% and Co-7% samples where they order due to the surface-strain bias resulting in the probe polarization anisotropy and the change of the sign of the $\mathcal{P}^-$-probe-polarization transients well above any transition at ∼110 and ∼70 K in the Co-5.1% and 7% samples, respectively [see Fig. 5(b)].

In the Co-11% sample, no probe polarization anisotropy is observed despite a clear indication of the pseudogap. However, the temperature dependence of the $\Delta R/R$ magnitude in this sample is very similar to the $\Delta R/R$ magnitude of the polarization-averaged $\Delta R/R$ transients in the Co-7% sample [see Fig. 5(b)] suggesting that the absence of the anisotropy is not due to the absence of nematic fluctuations, but due to the absence of their macroscopic ordering. The pseudogap can therefore be consistently associated with nematicity well into the overdoped region of the phase diagram.

A similar weak tetragonal symmetry breaking at high T extending well into the SC dome region of the phase diagram has been recently observed also in F doped Sm-1111 by high-resolution synchrotron powder diffraction.[58] This suggests that the presence of the nematic fluctuations is a general property of the electron doped FeAs planes.

D. Electron phonon coupling

1. *Determination of* $\lambda\langle\omega^2\rangle$

At room temperature, $Ba(Fe_{1-x}Co_x)_2As_2$ is a bad metal with resistivity in the sub-mΩcm range[33] and plasma frequency in an ∼1 eV range.[59,60] Since our data suggest that the effects of the nematic fluctuations become negligible around room temperature, we analyze the initial part of the $\Delta R/R$ transients at high T in the framework of the electron-phonon relaxation in metals.[61,62] The $\mathcal{F}$-independent relaxation at the room temperature [see Figs. 4(g) and 4(h)] warrants use of the low excitation expansion,[61] where in the high-temperature limit, the energy relaxation time is proportional to T,[61,62]

$$\tau = \frac{2\pi k_B T}{3\hbar\lambda\langle\omega^2\rangle}. \quad (7)$$

Here, $\lambda\langle\omega^2\rangle$ is the second moment of the Eliashberg function, $\alpha^2F(\omega)$, and k_B the Boltzman constant.[61] The equation is

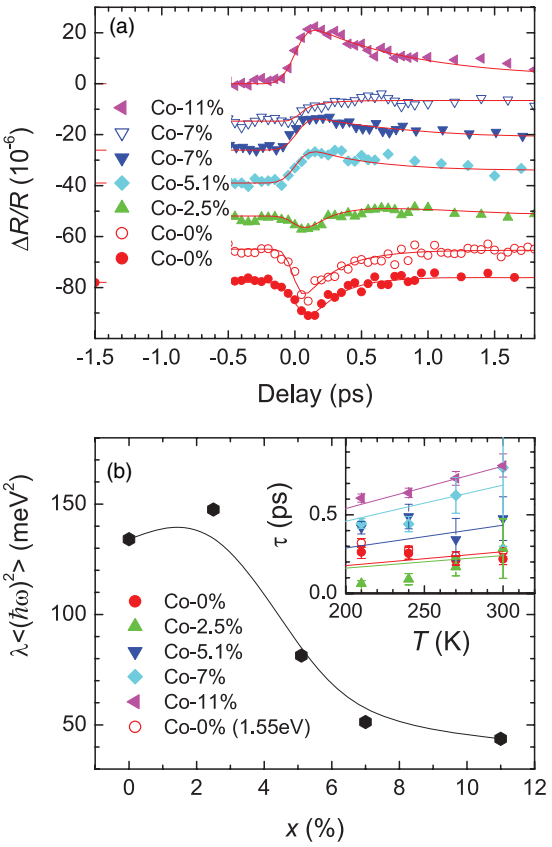

FIG. 11. (Color online) The initial part of $\Delta R/R$ transients at 300 K together with exponential fits as a function of Co doping (a). Open symbols correspond to the transients measured with 1.55 eV pump-photon energy in the Co-0% and Co-7% samples. The second moment of the Eliashberg function as a function of Co doping (b). The thin line is an eye guide. The T dependence of the initial relaxation time together with fits of Eq. (7) is shown in the inset.

expected to be valid for $k_BT > \hbar\omega_0$, where ω_0 is the characteristic Eliashberg-function phonon frequency. Estimating $\hbar\omega_0 \sim 20$ meV being a half of the maximum phonon frequency in $BaFe_2As_2$,[63] we expect Eq. (7) to be valid above ∼200 K.

We therefore determine the relaxation time above 200 K by fitting the initial part of the $\Delta R/R$ transients with a finite-rise-time single exponential decay similar to (2) [see Fig. 11(a)].[64] The temperature dependence of the relaxation time shows a clear linear T dependence predicted by Eq. (7) only in the near optimally doped Co-7% and overdoped Co-11% samples [see inset of Fig. 11(b)]. At lower Co dopings, there is a clear departure from the linear T dependence below ∼250 K indicating that ω_0 rises with decreasing Co doping and/or the effects of the nematic fluctuations can not be neglected up to ∼250 K.

In the non-SC samples, $\lambda\langle\omega^2\rangle$ is similar as in $SrFe_2As_2$ and SmAsFeO indicating a moderate electron phonon coupling constant $\lambda \sim 0.3$.[29] The value of $\lambda\langle\omega^2\rangle$ strongly drops in the superconducting samples consistent with high excitation density result.[31] The decrease of $\lambda\langle\omega^2\rangle$ with increasing Co doping [see Fig. 11(b)] suggests even lower $\lambda \sim 0.1$ in the SC samples, however, due to the decrease of ω_o the relative decrease of λ might be less than that of $\lambda\langle\omega^2\rangle$.

2. Possible multiband effects

Owing to the multiband nature of iron pnictides, it is possible that (due to optical selection rules) relaxation in some bands with possible higher couplings is not directly detected in $\Delta R/R$ transients. This would happen if the interband momentum scattering was slower than the energy relaxation rate in the unobserved band(s). The slow interband scattering rate possibility is suggested by the marked pump-photon energy dispersion of the Co-7% sample transients at high T [see Fig. 11(a)], which should be absent in the case of a very fast interband momentum scattering rate.

Trying to clarify this, we estimate the upper bound for the interband momentum scattering rate, $1/\tau_{IB}$, by the scattering rate of the narrow Drude peak.[60] From Ref. 60, we obtain $\tau_{IB} \gtrsim 1/30\,\mathrm{cm}^{-1} \sim 200$ fs, which is indeed comparable to the measured energy relaxation time [Fig. 11(b)] indicating a possibility that the estimated $\lambda\langle\omega^2\rangle$ is not well averaged over different bands. On the other hand, different analyses of the optical conductivity,[39,59,65,66] albeit in samples of different origin than ours,[67] result in a much broader Drude peak and consequently in, at least, ten times shorter τ_{IB} therefore supporting the fast interband momentum scattering rate scenario.

The observed pump-photon energy dispersion of the transients [see inset to Fig. 11(a)], which is negligible in the Co-0% sample, therefore suggests that $\lambda\langle\omega^2\rangle$ is well averaged over the bands in the undoped sample. This can not be claimed (due to the significant pump-photon energy dispersion in the Co-7% sample) for the samples with the Co doping well in the SC dome. Recent experiments with different pump/probe photon energies and better time resolution have, however, shown the presence of a faster relaxation component and consequently the presence of bands with $\lambda\langle\omega^2\rangle \sim 150$ meV^2 also in Co-7% and Co-11% samples.[68]

IV. SUMMARY AND CONCLUSIONS

We investigated doping dependence of electronic properties in $Ba(Fe_{1-x}Co_x)_2As_2$ by means of time resolved optical pump-probe spectroscopy. We observe a smooth evolution of the response with the Co doping as the system crosses over from the undoped SDW ground state to the superconducting ground state.

In the undoped and underdoped samples ($x \lesssim 5.1\%$), a clear signature of a bottleneck formation in the relaxation of the photoexcited QP is observed below the tetragonal to orthorhombic structural transition temperature T_s. The bottleneck is attributed to the partial charge gap opening due to the band-structure reconstruction below T_s, similar to other undoped iron pnictides.[29] The relative charge gap magnitude $2\Delta(0)/k_BT_s$ decreases with Co doping, consistent with a decrease of the stability of the orthorhombic/SDW state.

Similar to SmFeAs(O, F), we observe an anomalous T dependence of the relaxation in the normal state with the addition of the twofold rotational anisotropy in the tetragonal state. Although we were not able to determine the precise origin of the observed twofold rotational anisotropy, the observation of unidirectional terraces on the surface of the cleaved crystals suggests, that this anisotropy might be due to the anisotropic component of the surface strain induced by the laser heating. Since this strain is weak, this indicates a high susceptibility of the samples for fourfold to twofold rotational symmetry breaking consistent with a nematic order parameter. The anomalous normal state behavior is therefore tentatively attributed to electronic nematic fluctuations, that persist up to ~200 K, and open a pseudogap in the density of states near the Fermi energy. The fluctuation region extends well above T_s in the underdoped region and across all of the investigated SC dome region of the phase diagram. Due to the surface-strain bias, these fluctuations tend to align resulting in an anisotropic optical response also in the tetragonal near-optimally-doped 7%-Co sample.

Surprisingly, no clear separate anomaly is observed upon SDW formation at slightly lower T_{SDW} in underdoped samples ($x = 2.5\%$ and 5.1%). This suggests that the mechanism responsible for the pseudogap formation, nematic orbital fluctuations and partial gap opening below T_s is, despite the ubiquitous coupling to spins, not spin driven.

At room temperature, where the nematic fluctuations are negligible, the transients are analyzed in the framework of the Fermi-liquid electron-phonon relaxation model.[61] The analysis indicates, as in $SrFe_2As_2$ and SmAsFeO,[29] a moderate electron phonon coupling. The second moment of the Eliashberg function $\lambda\langle\omega^2\rangle$ is found to decrease with the Co doping resulting in a decrease of estimated λ from ~0.3 in the nonsuperconducting to ~0.1 in the superconducting samples. It is not clear, however, to what extent at higher Co dopings the systematic error due to a possible slow interband momentum scattering contributes to this decrease.

In the SC state, an additional relaxation component appears in the $\Delta R/R$ transients. The behavior of the SC component is consistent with isotropic SC gaps that have the BCS T dependence. The amplitude of the SC component saturates with increasing excitation density. The saturation is associated with a complete nonthermal destruction of the SC state, which proceeds on a sub-0.5-ps timescale.

In the near optimally doped sample with 7% Co doping ($T_c \sim 23$ K), the determined SC state optical destruction energy density, $U_p/k_B = 0.3$ K/Fe, is twice the thermodynamic condensation energy. A half of the deposited optical energy is therefore transferred to the low-frequency non-pair-breaking phonons on a sub-0.5-ps timescale. Comparison with SmFeAs(O, F)[26] ($T_c \sim 49$ K) indicates that U_p roughly scales as T_c^2. The SC state recovery dynamics in $Ba(Fe_{1-x}Co_x)_2As_2$ is slower than in SmFeAs(O, F) suggesting, contrary to SmFeAs(O, F), clean SC gaps in $Ba(Fe_{1-x}Co_x)_2As_2$.

ACKNOWLEDGMENTS

Work at Jozef Stefan Institute was supported by ARRS (Grant No. P1-0040). Work at Stanford University was supported by the Department of Energy, Office of Basic Energy Sciences under contract DE-AC02-76SF00515. We would like to thank M. Strojnik for help with AFM surface characterization and V. V. Kabanov for fruitful discussions.

[1] Y. Kamihara, H. Hiramatsu, M. Hirano, R. Kawamura, H. Yanagi, T. Kamiya, and H. Hosono, J. Am. Chem. Soc. **128**, 10012 (2006).

[2] Y. Kamihara *et al.*, J. Am. Chem. Soc. **130**, 3296 (2008).

[3] Z. Ren *et al.*, Europhys. Lett. **83**, 17002 (2008).

[4] R. H. Liu, G. Wu, T. Wu, D. F. Fang, H. Chen, S. Y. Li, K. Liu, Y. L. Xie, X. F. Wang, R. L. Yang, L. Ding, C. He, D. L. Feng, and X. H. Chen, Phys. Rev. Lett. **101**, 087001 (2008).

[5] K. Ahilan, F. L. Ning, T. Imai, A. S. Sefat, R. Jin, M. A. McGuire, B. C. Sales, and D. Mandrus, Phys. Rev. B **78**, 100501 (2008).

[6] F. Ning, K. Ahilan, T. Imai, A. S. Sefat, R. Jin, M. A. McGuire, B. C. Sales, and D. Mandrus, J. Phys. Soc. Jpn. **78**, 013711 (2009).

[7] C. Hess, A. Kondrat, A. Narduzzo, J. E. Hamann-Borrero, R. Klingeler, J. Werner, G. Behr, and B. Büchner, Europhys. Lett. **87**, 17005 (2009).

[8] E. E. M. Chia, D. Talbayev, J. X. Zhu, J. D. Thompson, A. J. Taylor, H. Q. Yuan, T. Park, C. Panagopoulos, G. F. Chen, J. L. Luo, and N. L. Wang, Phys. Rev. Lett. **102**, 117002 (2009).

[9] J.-H. Chu, J. G. Analytis, K. De Greve, P. L. McMahon, Z. Islam, Y. Yamamoto, and I. R. Fisher, Science **329**, 824 (2010).

[10] T.-M. Chuang, M. P. Allan, J. Lee, Y. Xie, N. Ni, S. L. Bud'ko, G. S. Boebinger, P. C. Canfield, and J. C. Davis, Science **327**, 181 (2010).

[11] M. A. Tanatar, N. Ni, A. Thaler, S. L. Bud'ko, P. C. Canfield, and R. Prozorov, Phys. Rev. B **82**, 134528 (2010).

[12] A. Dusza, A. Lucarelli, F. Pfuner, J.-H. Chu, I. R. Fisher, and L. Degiorgi, Europhys. Lett. **93**, 37002 (2011).

[13] M. A. Tanatar, E. C. Blomberg, A. Kreyssig, M. G. Kim, N. Ni, A. Thaler, S. L. Bud'ko, P. C. Canfield, A. I. Goldman, I. I. Mazin, and R. Prozorov, Phys. Rev. B **81**, 184508 (2010).

[14] J. J. Ying, X. F. Wang, T. Wu, Z. J. Xiang, R. H. Liu, Y. J. Yan, A. F. Wang, M. Zhang, G. J. Ye, P. Cheng, J. P. Hu, and X. H. Chen, Phys. Rev. Lett. **107**, 067001 (2011).

[15] M. Yi, D. Lu, J.-H. Chu, J. G. Analytis, A. P. Sorini, A. F. Kemper, B. Moritz, S.-K. Mo, R. G. Moore, M. Hashimoto, W.-S. Lee, Z. Hussain, T. P. Devereaux, I. R. Fisher, and Z.-X. Shen, Proc. Natl. Acad. Sci. USA **108**, 6878 (2011).

[16] F. Rullier-Albenque, D. Colson, A. Forget, and H. Alloul, Phys. Rev. Lett. **103**, 057001 (2009).

[17] H.-S. Lee, M. Bartkowiak, J.-H. Park, J.-Y. Lee, J.-Y. Kim, N.-H. Sung, B. K. Cho, C.-U. Jung, J. S. Kim, and H.-J. Lee, Phys. Rev. B **80**, 144512 (2009).

[18] J. Demsar, B. Podobnik, V. V. Kabanov, T. Wolf, and D. Mihailovic, Phys. Rev. Lett. **82**, 4918 (1999).

[19] R. Kaindl, M. Woerner, T. Elsaesser, D. Smith, J. Ryan, G. Farnan, M. McCurry, and D. Walmsley, Science **287**, 470 (2000).

[20] R. D. Averitt, G. Rodriguez, A. I. Lobad, J. L. W. Siders, S. A. Trugman, and A. J. Taylor, Phys. Rev. B **63**, 140502 (2001).

[21] G. P. Segre, N. Gedik, J. Orenstein, D. A. Bonn, R. Liang, and W. N. Hardy, Phys. Rev. Lett. **88**, 137001 (2002).

[22] P. Kusar, J. Demsar, D. Mihailovic, and S. Sugai, Phys. Rev. B **72**, 014544 (2005).

[23] Y. H. Liu, Y. Toda, K. Shimatake, N. Momono, M. Oda, and M. Ido, Phys. Rev. Lett. **101**, 137003 (2008).

[24] C. Ning, W. Yan-Feng, Z. Ji-Min, Z. Shi-Ping, Y. Qian-Sheng, Z. Zhi-Guo, and F. Pan-Ming, Chin. Phys. Lett. **25**, 2257 (2008).

[25] T. Mertelj, V. Kabanov, C. Gadermaier, N. Zhigadlo, S. Katrych, Z. Bukowski, J. Karpinski, and D. Mihailovic, J. Supercond. Novel Magn. **22**, 575 (2009).

[26] T. Mertelj, P. Kusar, V. V. Kabanov, L. Stojchevska, N. D. Zhigadlo, S. Katrych, Z. Bukowski, J. Karpinski, S. Weyeneth, and D. Mihailovic, Phys. Rev. B **81**, 224504 (2010).

[27] D. H. Torchinsky, G. F. Chen, J. L. Luo, N. L. Wang, and N. Gedik, Phys. Rev. Lett. **105**, 027005 (2010).

[28] E. E. M. Chia, D. Talbayev, J.-X. Zhu, H. Q. Yuan, T. Park, J. D. Thompson, C. Panagopoulos, G. F. Chen, J. L. Luo, N. L. Wang, and A. J. Taylor, Phys. Rev. Lett. **104**, 027003 (2010).

[29] L. Stojchevska, P. Kusar, T. Mertelj, V. V. Kabanov, X. Lin, G. H. Cao, Z. A. Xu, and D. Mihailovic, Phys. Rev. B **82**, 012505 (2010).

[30] Y. Gong, W. Lai, T. Nosach, L. J. Li, G. H. Cao, Z. A. Xu, and Y. H. Ren, New J. Phys. **12**, 123003 (2010).

[31] B. Mansart, D. Boschetto, A. Savoia, F. Rullier-Albenque, F. Bouquet, E. Papalazarou, A. Forget, D. Colson, A. Rousse, and M. Marsi, Phys. Rev. B **82**, 024513 (2010).

[32] D. H. Torchinsky, J. W. McIver, D. Hsieh, G. F. Chen, J. L. Luo, N. L. Wang, and N. Gedik, Phys. Rev. B **84**, 104518 (2011).

[33] J.-H. Chu, J. G. Analytis, C. Kucharczyk, and I. R. Fisher, Phys. Rev. B **79**, 014506 (2009).

[34] C. Lester, J.-H. Chu, J. G. Analytis, S. C. Capelli, A. S. Erickson, C. L. Condron, M. F. Toney, I. R. Fisher, and S. M. Hayden, Phys. Rev. B **79**, 144523 (2009).

[35] We observed no pump polarization dependence of the response at fixed probe polarization.

[36] P. Kusar, V. V. Kabanov, S. Sugai, J. Demsar, T. Mertelj, S. Sugai, and D. Mihailovic, Phys. Rev. Lett. **101**, 227001 (2008).

[37] The detailed homogeneity analysis of samples was published elsewhere (see Ref. 33).

[38] The critical temperature was determined from our optical measurements based on the sample holder temperature and is apparently lower than the phase diagram [see Fig. 2(e)] value due to the sample heating by the laser.

[39] N. Barišić, D. Wu, M. Dressel, L. J. Li, G. H. Cao, and Z. A. Xu, Phys. Rev. B **82**, 054518 (2010).

[40] We calculated U_c from the heat capacity data in Ref. 44.

[41] L. Stojchevska, P. Kusar, T. Mertelj, V. V. Kabanov, Y. Toda, X. Yao, and D. Mihailovic, Phys. Rev. B **84**, 180507 (2011).

[42] The weak nonmonotonic temporal dependence of the SC component during the plateau could not be reliably identified as an intrinsic effect and is attributed to a weak T dependence of the subtracted normal state response.

[43] D. C. Mattis and J. Bardeen, Phys. Rev. **111**, 412 (1958).

[44] F. Hardy, P. Burger, T. Wolf, R. A. Fisher, P. Schweiss, P. Adelmann, R. Heid, R. Fromknecht, R. Eder, D. Ernst, H. v. Löhneysen, and C. Meingast, Europhys. Lett. **91**, 47008 (2010).

[45] M. Tropeano, A. Martinelli, A. Palenzona, E. Bellingeri, E. GalleanidAgliano, T. D. Nguyen, M. Affronte, and M. Putti, Phys. Rev. B **78**, 094518 (2008).

[46] D. Mihailovic and J. Demsar, *Spectroscopy of Superconducting Materials* (American Chemical Society: Washington, DC, 1999), Chap. Time-resolved optical studies of quasiparticle dynamics in high-temperature superconductors, pp. 230–244.

[47] L. Rettig, R. Cortés, S. Thirupathaiah, P. Gegenwart, H. S. Jeevan, M. Wolf, J. Fink, and U. Bovensiepen, Phys. Rev. Lett. **108**, 097002 (2012).

[48] Due to the presence of the surface-strain bias the transition is, strictly speaking, a crossover (see Ref. 9).

[49] The apparent peak of τ_B at T_c in the Co-7% sample is due to the appearance of the SC relaxation component.

[50]At high temperature, it is strongly influenced by the acoustic wave feature around the 10 ps delay.
[51]The SC component shows the same T dependence for both polarizations consistent with isotropic SC gaps.
[52]D. Dvorsek, V. V. Kabanov, J. Demsar, S. M. Kazakov, J. Karpinski, and D. Mihailovic, Phys. Rev. B **66**, 020510 (2002).
[53]V. V. Kabanov, J. Demsar, B. Podobnik, and D. Mihailovic, Phys. Rev. B **59**, 1497 (1999).
[54]J. G. Analytis, R. D. McDonald, J. H. Chu, S. C. Riggs, A. F. Bangura, C. Kucharczyk, M. Johannes, and I. R. Fisher, Phys. Rev. B **80**, 064507 (2009).
[55]T. Dong, Z. G. Chen, R. H. Yuan, B. F. Hu, B. Cheng, and N. L. Wang, Phys. Rev. B **82**, 054522 (2010).
[56]The T dependence of the $\mathcal{P}^{-}\Delta R/R$ magnitude is qualitatively similar with an offset due to another relaxation process.
[57]E. Fradkin, S. A. Kivelson, M. J. Lawler, J. P. Eisenstein, and A. P. Mackenzie, Annual Review of Condensed Matter Physics **1**, 153 (2010).
[58]A. Martinelli, A. Palenzona, M. Tropeano, M. Putti, C. Ferdeghini, G. Profeta, and E. Emerich, Phys. Rev. Lett. **106**, 227001 (2011).
[59]W. Z. Hu, J. Dong, G. Li, Z. Li, P. Zheng, G. F. Chen, J. L. Luo, and N. L. Wang, Phys. Rev. Lett. **101**, 257005 (2008).
[60]A. Lucarelli, A. Dusza, F. Pfuner, P. Lerch, J. G. Analytis, J.-H. Chu, I. R. Fisher, and L. Degiorgi, New J. Phys. **12**, 073036 (2010).
[61]V. V. Kabanov and A. S. Alexandrov, Phys. Rev. B **78**, 174514 (2008).
[62]C. Gadermaier, A. S. Alexandrov, V. V. Kabanov, P. Kusar, T. Mertelj, X. Yao, C. Manzoni, D. Brida, G. Cerullo, and D. Mihailovic, Phys. Rev. Lett. **105**, 257001 (2010).
[63]R. Mittal, Y. Su, S. Rols, T. Chatterji, S. L. Chaplot, H. Schober, M. Rotter, D. Johrendt, and T. Brueckel, Phys. Rev. B **78**, 104514 (2008).
[64]The Co-2.5% sample shows a clear two component initial decay at the room temperature so a two exponential fits were used.
[65]J. J. Tu, J. Li, W. Liu, A. Punnoose, Y. Gong, Y. H. Ren, L. J. Li, G. H. Cao, Z. A. Xu, and C. C. Homes, Phys. Rev. B **82**, 174509 (2010).
[66]M. Nakajima, S. Ishida, K. Kihou, Y. Tomioka, T. Ito, Y. Yoshida, C. H. Lee, H. Kito, A. Iyo, H. Eisaki, K. M. Kojima, and S. Uchida, Phys. Rev. B **81**, 104528 (2010).
[67]Our samples have the same origin as in Ref. 60 and $1/\tau_{IB}$ can be strongly affected by impurities.
[68]C. Gadermaier *et al*., arXiv:1205.4978 (2012).